Journal of Engineering and Technological Sciences

Research Paper

Chloride Salt-Intercalated Ti2C Membranes for Ultraquick Cationic Dye Removal

Fuja Sagita[1], Kholifatul Mukhoibibah[1], & Grandprix T.M. Kadja[1,2,*]

[1]Division of Inorganic and Physical Chemistry, Faculty of Mathematics and Natural Sciences, Institut Teknologi Bandung, Jalan Ganesa No. 10, Bandung 40132, Indonesia
[2]Research Center for Nanosciences and Nanotechnology, Institut Teknologi Bandung, Jalan Ganesa No. 10, Bandung 40132, Indonesia

*Corresponding author: grandprix.thomryes@itb.ac.id

Abstract

Ti_2C is a 2D nanomaterial with an ultrathin layered structure. This material has remarkable properties due to the –O, –F, and –OH functional groups in surface termination, which makes it hydrophilic and suitable for membrane applications. Herein, we reported the chloride salt-intercalated Ti_2C membrane for methylene blue (MB) removal. The modification was done by a simple mixing method between chloride salt and Ti_2C. First, Ti_2C was synthesized from its parent phase of Ti_2AlC using in-situ HF etchant. Then, Ti_2C was modified using chloride salt (NaCl, KCl, $MgCl_2$, and $CaCl_2$), and mixed cellulose ester (MCE) was used as a membrane support to produce a MXene-based membrane (MXM). The results show that chloride salt ions enhance the interlayer spacing of Ti_2C due to the ability of salt cation to be inserted and replace the Li^+ as intercalant. This result is also evidenced by the difference in *d*-spacing in XRD analysis. In methylene blue removal, the flux of the membrane was excellent, around 2000-3000 L m^{-2} h^{-1}, with a dye removal value above 97%. The high dye removal is correlated with the electrostatic interaction between the negative surface of Ti_2C and the positive charge of MB. Then, the remarkable performance was reached by MXM-KCl with flux and rejection of 3303.31 L m^{-2} h^{-1} and 99.01%, respectively. The excellent flux of MXM-KCl correlated with the Gibbs free energy hydration of K^+ is lower than the other salt cations (Na^+, Mg^{2+}, and Ca^{2+}). In addition, all membranes exhibit great fouling resistance, with an FRR value of about 90%.

Keywords: *intercalant; membranes; methylene blue; MXene; salt; Ti2C.*

Introduction

Methylene blue (MB) is a synthetic dye commonly used in industry for various applications, such as coloring paper, wool dyeing, hair coloring agents, and redox reaction indicators (Din et al., 2021; Kumar et al., 2024). Besides that, the typical redox features of MB can be used in biomedical as a biological stain (Kumar et al., 2024). MB dissolved in water will absorb and reflect the sunlight, which impedes the sunlight from reaching the aquatic environment (Haider et al., 2022). Nevertheless, the excessive use of MB is unfavorable for the environment and living things. MB can induce several diseases in humans, such as jaundice, vomiting, dizziness, and methemoglobinemia (Kishor et al., 2021; Kumar et al., 2024; Oladoye et al., 2022). MB does not degrade naturally, and the structure is relatively stable (Kumar et al., 2024; Oladoye et al., 2022). Thus, finding a more appropriate strategy for MB degradation is urgently required. There are several ways to remove dyes in the aquatic environment, such as physical adsorption, biological degradation, oxidation, reduction, and bio-adsorbent (Kumar et al., 2024; Manzoor et al., 2024; Naseem et al., 2023, 2024). However, these methods have several limitations, such as contaminants from secondary metal ions, sludge disposal issues, and unreasonable expense (Gautam et al., 2020; Jabbar et al., 2023; Priyadharsini et al., 2023). Membrane technology has gained substantial attention due to numerous benefits, including no change in chemical phase, ease of control, cost-effectiveness, and low energy consumption (Kadja et al., 2023; Sagita et al., 2024; Umam et al., 2023; Zhao et al., 2021). There are two types of membranes based on material source, i.e., inorganic and organic materials (Zafar et al., 2024). In its application, the researcher produces a hybrid membrane that is a mixture of inorganic and organic materials to enhance its performance(Zheng et al., 2024).

Two-dimensional materials have commonly been explored in membranes, such as hexagonal boron nitride, metal-organic frameworks (MOFs), graphitic carbon nitride, and metal, carbide, or carbonitride (MXene) (Al-Hamadani et al., 2020; Karahan et al., 2020). MXene is a new 2D ultrathin nanomaterial with the general formula $M_{n+1}X_nT_x$, where M and

Copyright by authors ©2026 Published by IRCS - ITB
ISSN: 2337-5779
J. Eng. Technol. Sci. Vol. 58, No. 4, 2026, 475-484
DOI: 10.5614/j.eng.technol.sci.2026.58.4.1

X are early transition metals and carbide and/or nitride, respectively. At the same time, T_x is called terminal functional groups, e.g., –OH, –F, and O (Berdiyorov & Mahmoud, 2017; Gogotsi & Anasori, 2019; Halim et al., 2019; L. Li et al., 2017; Naguib et al., 2011). The hydrophilic surface of MXene and its layered structure are favorable features for membrane applications. Moreover, MXene has an outstanding structure, large surface area, and charge-selective sieving (Berdiyorov & Mahmoud, 2017; Ibrahim et al., 2022). Several researchers studied different MXene applications in membranes, such as Ti_3C_2, V_2C, and V_4C_3 (Lan et al., 2022; Zhang et al., 2019). For instance, Wei et al. (Wei et al., 2019) prepared a graphene oxide-Ti_3C_2 composite membrane for MB removal. Adding Ti_3C_2 could increase the interlayer spacing of the membrane more than pure graphene oxide, elevating the membrane's performance (rejection of 98.56% and flux of 16.69 L m^{-2} h^{-1}). In another previous work, salt-modified Ti_3C_2-based membranes were prepared to boost membrane performance in terms of both selectivity and permeability. Modifying Ti_3C_2-based membrane with KCl has an exceptional flux and rejection of 141 L m^{-2} h^{-1} and ~100%, respectively (Sagita et al., 2022).

This study investigated the synthesis and the application of Ti_2C for MB removal by using mixed cellulose ester (MCE) as a supporting membrane. In-situ HF etchant was used to transform the Ti_2AlC phase to Ti_2C by removing the Al layer. Several characterizations were applied to reveal the Ti_2C product, such as X-ray diffraction (XRD), Raman, and scanning Electron microscopy (SEM) equipped with energy-dispersive X-ray spectroscopy (EDX). Then, the Ti_2C-based membrane was formed by depositing Ti_2C into a supported membrane. Furthermore, the membranes were modified using chloride salt (NaCl, KCl, $MgCl_2$, and $CaCl_2$). The Ti_2C-based membrane possessed the typical layered structure, with the interlayer spacing changing along with the modification. Then, a series of membrane performance tests was conducted using facile vacuum filtration. As a result, the Ti_2C-based membrane with and without modification showed outstanding properties, leading to excellent separation performance.

Materials and Methods

Materials

The chemical used in this study is Ti_2AlC (MAX, China), lithium fluoride (LiF 99.99%, Merck, USA), hydrochloric acid (HCl 37%, Merck, Germany), ethanol (C_2H_5OH, Supelco, Germany), aqua DM, dimethyl sulfoxide (Supelco, Japan), methylene blue (Mw 319.85 g mol^{-1}, Merck, Germany), potassium chloride (KCl Mw 75.55 g mol^{-1}, Merck, Germany), sodium chloride (NaCl Mw 58.44 g mol^{-1}, Merck, Germany), and $MgCl_2.6H_2O$ (Mw 203.31 g mol^{-1}, Sigma Aldrich, Canada), $CaCl_2.2H_2O$ (Mw 147.01 g mol^{-1}). Mixed cellulose ester (MCE) was purchased from Green Mall with a mean pore diameter and diameter of 0.22 µm and 4.7 cm, respectively.

Synthesis of MXene

Ti_2C was produced by etching the Al layer from its parent compound of Ti_2AlC using in-situ HF. First, 1.10 g of LiF was dissolved into 30 mL of HCl 6 M with stirring for 10 min. Then, 1 g of Ti_2AlC was gradually added to the mixture and reacted at 40℃ for 36 h. The produced mixture was centrifuged for 5 min at 3500 rpm. After that, the solid was collected and washed with deaeration ethanol and water four times at 3500 rpm until it reached pH 5. The solid was accumulated and dried at room temperature. Finally, the powder was dissolved into Aqua DM and sonicated for 1.50 h. The resulting dispersion is Ti_2C.

Membrane Preparation and Modification

Mixed-cellulose ester (MCE) was used as a solid support membrane. First, Ti_2C was deposited on MCE using vacuum-assisted filtration, with a total loading concentration of 1 mg cm^{-2}, 2 mg cm^{-2}, and 3 mg cm^{-2}. This result is labeled MXM. Furthermore, MXM was modified with chloride salt by adding the mixed solution of 20 mL of MXene and 1 M chloride salt in a ratio of 1:1. Then, the mixture was genuinely poured and deposited on MCE. The resulting membrane is marked as MXM-S, with S stands for chloride salt ($CaCl_2$, $MgCl_2$, KCl, and NaCl), and MXM is a pure MXene-based membrane.

Membrane Characterization

Several characterizations were used in this study. First, X-ray diffraction (XRD) analysis over a 2θ range of 5°-90°, the step size was 0.02° (Cu-Kα radiation, λ = 1.54 Å), was recorded using Bruker D8 Advance. Then, scanning electron microscopy (SEM) images of samples were taken with FESEM Thermo Scientific Quattro S equipped with energy-dispersive X-ray spectroscopy (EDX). A Horiba LabRAM HR Evolution spectrometer was used to analyze the Ti2C and Ti2AlC Raman shifted. The analysis was conducted using a 532 nm laser at a power output of 10 mW. Then, the FTIR spectra were obtained using a Bruker Alpha FTIR (Wavenumber from 4000 cm-1 to 500 cm-1). Furthermore, the hydrophilicity of

DOI: 10.5614/j.eng.technol.sci.2026.58.4.1

membranes was obtained using water contact angle analysis, which was measured by dropping water on the membrane surface.

Membrane Filtration Test

The resulting MXM and MXM-S were used for methylene blue (MB) filtration, which was performed using a facile vacuum filtration. The MB feed concentration was 100 mg L^{-1}. The initial and final concentration of MB was measured using a UV-vis spectrophotometer at λ = 663 nm. The following equation (Eqs. (1) & (2))was used to calculate the rejection (R) and dye flux (J):

$$R = (1 - \frac{C_p}{C_f}) \quad (1)$$

$$J = \frac{V}{t\,A} \quad (2)$$

C_p (mg L^{-1}) is the permeate concentration, while C_f (mg L^{-1}) is the feed concentration of MB solution. Next, A is an effective membrane area (m^2), V is a permeate volume (L), and t is filtration times (h). The total volume of the feed solution is 10 mL for all membrane tests. Furthermore, antifouling of the membrane was obtained by calculating the flux recovery ratio (FRR) as follows in Eq. (3):

$$FRR = \frac{J_R}{J_w}\ x\ 100\% \quad (3)$$

J_R and J_w are flux after dye filtration and flux of pure water.

Results

Ti_2C has been successfully synthesized from the MAX phase of Ti_2AlC via etching Al layer using in situ HF. Figure 1(a) shows the XRD diffractogram of Ti_2C and Ti_2AlC. Meanwhile, the XRD of Ti_2C with salt modification was depicted in Figure 1(b). Moreover, the Raman analysis (Figure 1c) shows the characteristic peak related to the Ti_2C and Ti_2AlC. FTIR spectra of all samples are shown in Figure 1(d). MXM and MXM-S have a broad peak at 3272 $cm^{-1,}$ which is correlated with O-H stretching, while this peak disappears in Ti_2AlC (H. Ahmad et al., 2023). In addition, the other peaks at 1632 cm^{-1} (O-H bending) and 564 cm^{-1} (Ti-O bending) can be observed in MXM and MXM-S, which indicates the terminal functional group of Ti_2C (H. Ahmad et al., 2023; Y. Li et al., 2017). The morphological images of membranes were taken using scanning electron microscopy (SEM) (Figure 2(a), (b)). This characterization plays an essential role in this study to determine the accomplishment of the synthesis. Moreover, the MXM-S have been analyzed using SEM coupling with EDX, as shown in Figure 3 (a) and (b).

The Ti_2C has terminal functional groups, *i.e.,* –O, –OH, and –F, which cause its hydrophilic nature. This feature is beneficial for membrane applications. Thus, water contact angle (WCA) analysis is indispensable to determine the membrane hydrophilicity. Figure 4(a) depicts the WCA of all membranes. The filtration test of MXM and MXM-S samples was applied in methylene blue removal. The loading amount of Ti_2C has been varied. As shown in Figure S5, the difference in Ti_2C loading amount will generate different membrane performance. Figure 4(b) shows the flux and dye removal of all membranes. In this study, there are two types of chloride, i.e., chloride salt with a cation charge of +1 (NaCl and KCl) and +2 ($MgCl_2$ and $CaCl_2$). Pristine MXM has a flux of 2680.19 L m^{-2} h^{-1}, while the chloride MXM-S has a more excellent flux value (MXM-NaCl= 2809.76 L m^{-2} h^{-1}, MXM-KCl = 3303.31 L m^{-2} h^{-1}, MXM-$MgCl_2$ = 2829.13 L m^{-2} h^{-1}, MXM-$CaCl_2$ = 3000.16 L m^{-2} h^{-1}). Fouling is also critical to the membrane application because it can affect the membrane's performance. The flux recovery ratio (FRR) is a parameter that indicates membrane fouling. The FRR of membranes is shown in Figure 4(c), which is the antifouling of all membranes relatively high.

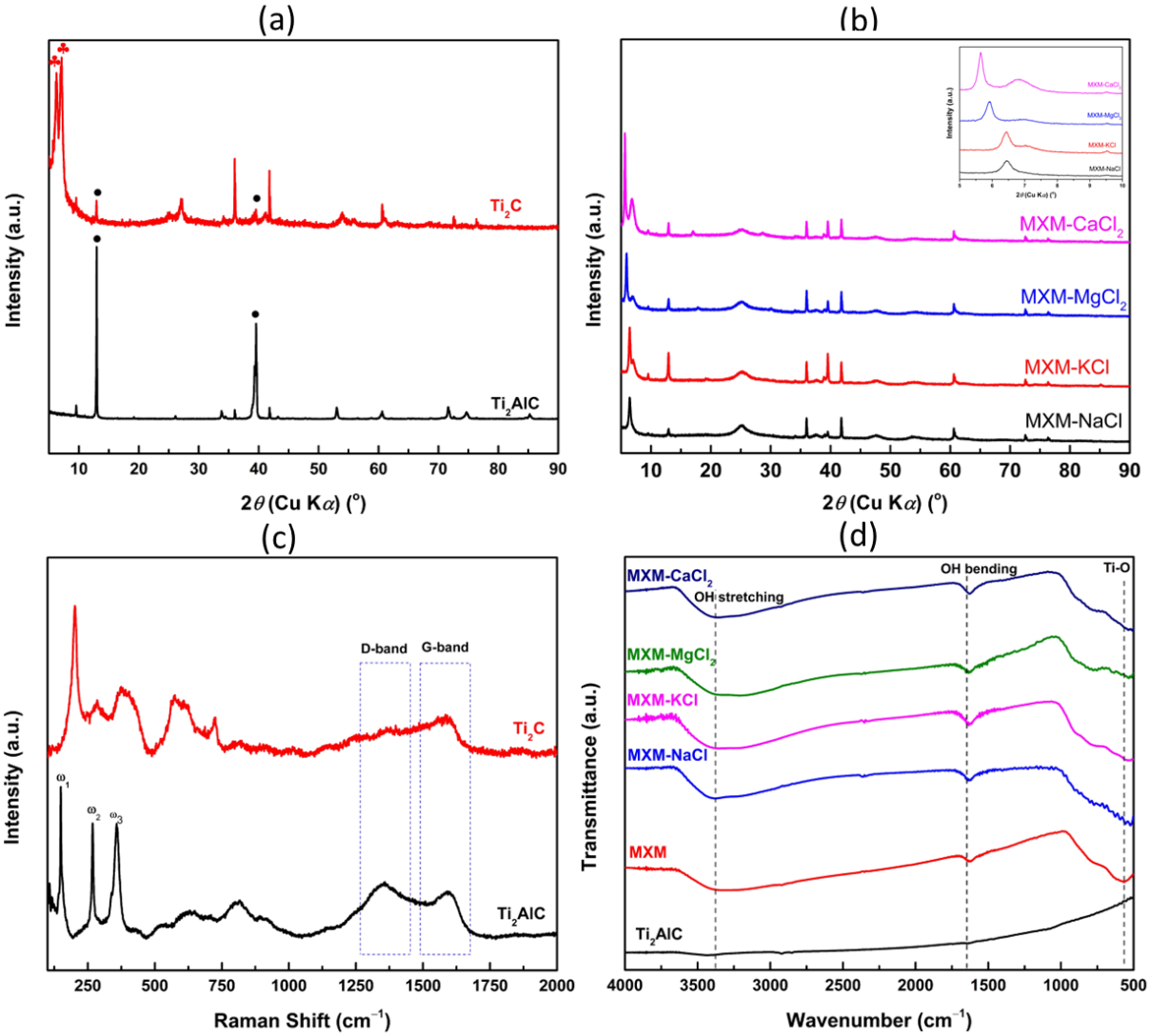

Figure 1 (a) XRD pattern of Ti_2AlC and Ti_2C, (b) XRD pattern of chloride salt-modified Ti_2C, (c) Raman spectra of Ti_2AlC and Ti_2C, and (d) FTIR spectra of all membranes and Ti_2AlC.

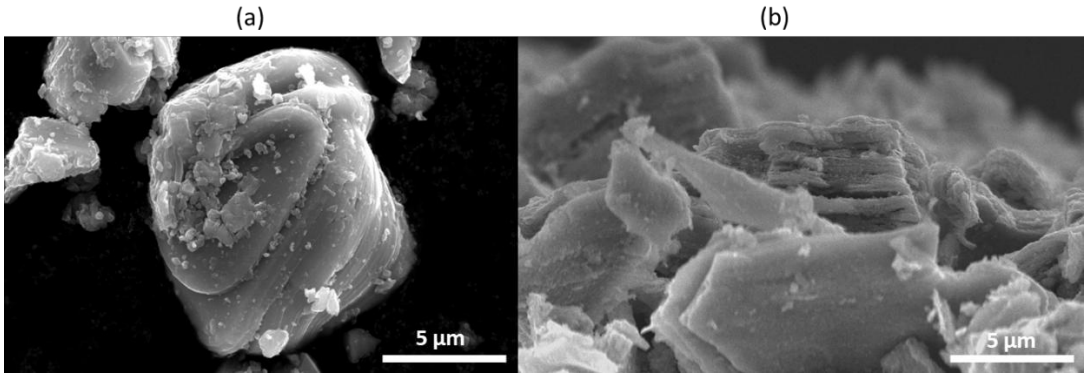

Figure 2 SEM images of (a) Ti_2AlC and (b) Ti_2C.

DOI: 10.5614/j.eng.technol.sci.2026.58.4.1

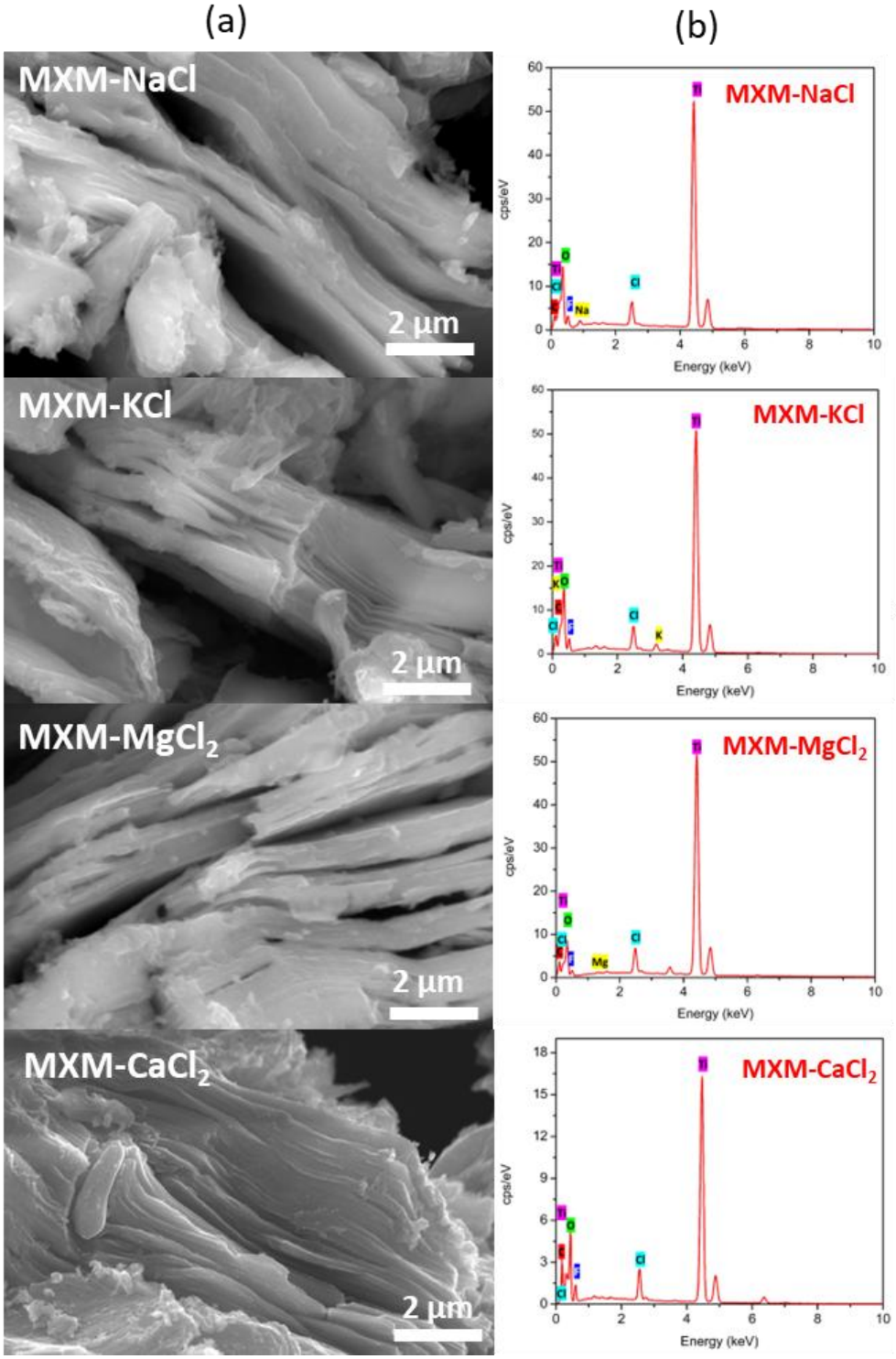

Figure 3 (a) SEM images and (b) EDX spectra of MXM-S sample.

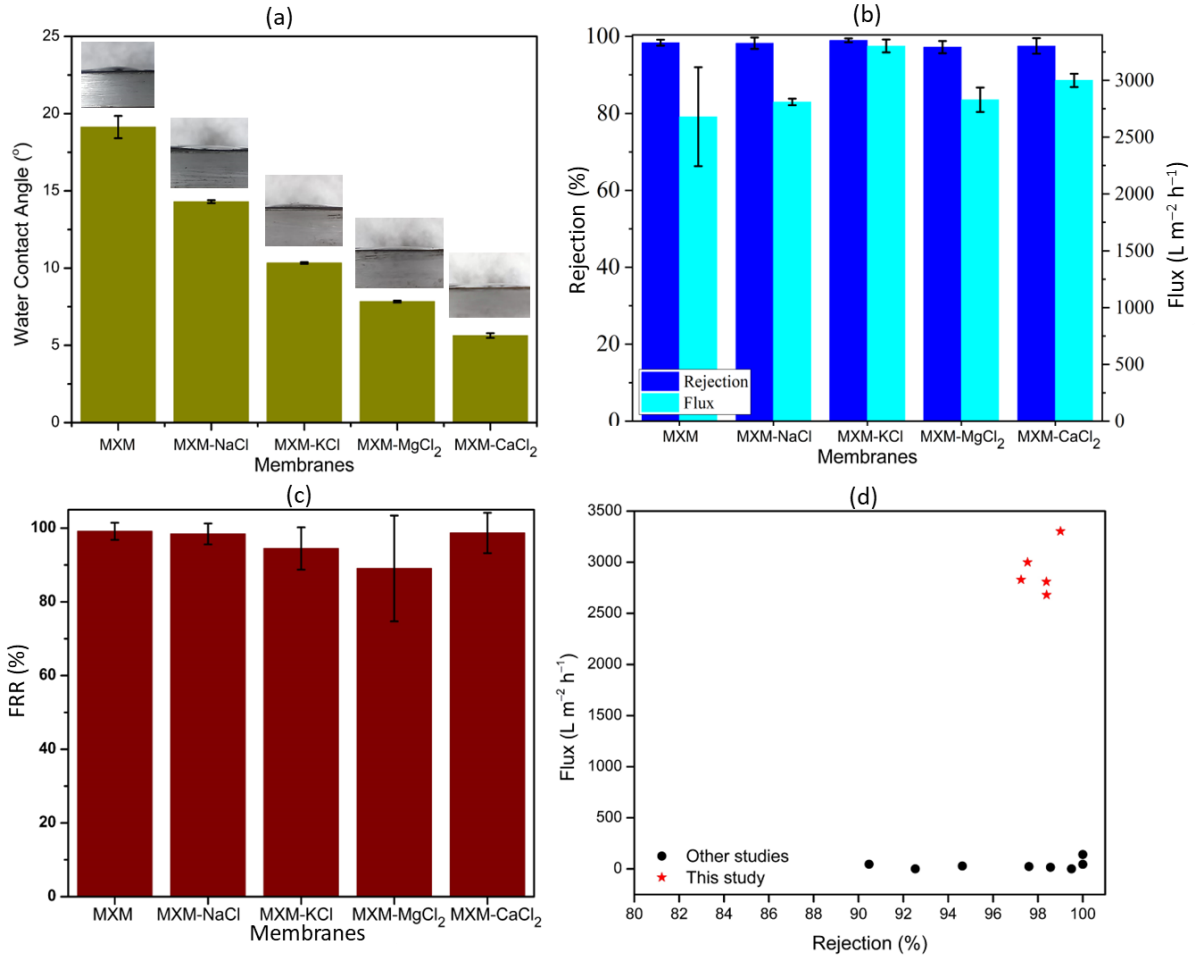

Figure 4 (a) Water contact angle trend, (b) flux and rejection, (c) FRR of MXM and MXM-S samples, and (d) filtration performance of this study and others.

Discussion

Ti_2AlC has major features at 2θ 12.97° and 39.57°, correlating with the (002) plane and Al peaks, respectively (Melchior et al., 2018). In Ti_2C, the peak of Al disappeared, indicating that the removal of the Al atom was successful. Meanwhile, the (002) peak still exists and shifts into two minor peaks, 2θ *6.25*° and 7.11°. This shift demonstrates an increase in the *d*-spacing of Ti_2C. Furthermore, the use of chloride salts in Ti_2C has replaced Li^+ as an intercalant. In addition, the d-spacing of Ti_2C with salt modification increases. This can be observed from the shift of the (002) plane to 6.46°, 6.42°, 5.91°, and 5.65° for MXM-NaCl, MXM-KCl, MXM-$MgCl_2$, and MXM-$CaCl_2$, respectively.

Raman analysis demonstrates the main features of Ti_2AlC at ω_1, ω_2, and ω_3, with Raman shifts at 149 cm^{-1}, 267 cm^{-1}, and 360 cm^{-1}, respectively (Melchior et al., 2018). These peaks are assigned to Ti and Al's shear and longitudinal vibration. The absence of these peaks in the Ti_2C spectrum indicates the successful removal of the Al layer in the Ti_2AlC phase. In addition, new peaks are apparent at 1350 cm^{-1} and 1580 cm^{-1} in the Raman spectra of Ti_2C assigned to the D-band and G-band, respectively (Melchior et al., 2018; Sagita et al., 2022). The D-band is associated with perturbed sp^2, while the G-band is ascribed to stretching the C-C bond in sp^2, both in chains and rings. The D-band and G-band imply the existence of amorphous carbon in Ti_2C. FTIR analysis shows that the addition of chloride salt does not change the terminal functional group of Ti_2C.

Morphological analysis shows that Ti_2AlC has a denser and more compact structure compared to Ti_2C. The Ti_2AlC bulk (3D structure) was successfully transformed into Ti_2C layered structure (2D structure) using HF treatment. In addition, Ti_2C has a space between the layers of Ti_2C due to the removal of the Al atom from Ti_2AlC. SEM EDX analysis demonstrates that All MXM-S have a typical morphology like Ti_2C. On the other hand, all MXM-S have different EDX spectra depending on the type of salt used to modify them. However, each MXM and MXM-S sample has F, O, C, and Ti atoms, which are the primary atoms in Ti_2C. The O and F atoms appear due to their roles as terminal functional groups

DOI: 10.5614/j.eng.technol.sci.2026.58.4.1

of Ti_2C. The peak of Al also disappears, indicating that the etching process was successful. Figures S1-S4 depict the EDX mapping of the MXM-S samples in which the atoms of samples are evenly distributed in the membrane. As a result, the EDX analysis also demonstrated that the cation of salt replaced the Li^+ as intercalant.

Water contact angle analysis shows that adding chloride salts increases hydrophilicity, denoted by a successive decrease in the water contact angle. The chloride salt ion can be present in the surface layer of Ti_2C, which can interact with water via ion-dipole interaction. Hence, the interaction between MXM-S and water is higher than pure MXM and water. Further analysis on the effect of Ti_2C loading was observed. Results shows that the greater the amount of Ti_2C used, the thicker the Ti_2C layer on the membrane will be, resulting in a lower flux. This is because the path passed by the feed will be longer. The membrane flux will decrease due to the high loading amount of Ti_2C. Conversely, the high loading amount of Ti_2C is beneficial because it generates high rejection values. The high loading amount of Ti_2C will provide many active surfaces of Ti_2C, which can enhance membrane rejection. As a result, 3 mg cm^{-2} of Ti_2C exhibits the best performance. Therefore, this loading amount is used in the MXM and MXM-S. As mentioned before, the modification with chloride salt could change the *d*-spacing and interlayer spacing of the membrane. As a result, MXM and MXM-S have a flux over 2000 m^{-2} h^{-1}, indicating the membrane's superior permeability.

In terms of flux evaluation, the chloride salt generally boosts the membrane flux. For chloride salt, with a cation charge of +1, the trend of flux is MXM-KCl > MXM-NaCl > MXM, while the flux trend of the membrane with a cation charge of +2 is MXM-$CaCl_2$ > MXM-$MgCl_2$. Moreover, the increasing flux of MXM-S is influenced by the cation and anion inserted between the Ti_2C layers. The chloride salt cations can interact with water molecules, which is the solvent of the feed solution. Each ion has a different Gibbs free energy hydration as follows: ΔG_{hyd} Li^+ = −566.59 kJ mol^{-1}, ΔG_{hyd} Na^+ = −365.01 kJ mol^{-1}, ΔG_{hyd} K^+ = −295.21 kJ mol^{-1}, ΔG_{hyd} Mg^{2+} = −1831.22 kJ mol^{-1}, ΔG_{hyd} Ca^{2+} = −1493.00 kJ mol^{-1}, and ΔG_{hyd} Cl^- = −310.54 kJ mol^{-1}) (Adapa & Malani, 2018; J. Li & Wang, 2017; Schmid et al., 2000). The MXM-KCl has a higher flux, which means faster water transport than the others because it has a lower Gibbs free energy hydration (Sagita et al., 2022). Thus, the interaction between KCl and water as a solvent feed solution is relatively weak. Furthermore, all membrane samples have an excellent dye removal of about >97%. The chloride salt modification does not influence the dye removal performance. Dye removal of MXM, MXM-NaCl, MXM-KCl, MXM-$MgCl_2$, and MXM-$CaCl_2$ are 98.39%, 98.28%, 99.01%, 97.25%, and 97.54%, respectively. The higher rejection of all membranes is due to the electrostatic interaction between Ti_2C surface and MB, in which the surface of Ti_2C has a relatively negative charge, and MB is fairly positive. This is proven by the zeta potential analysis, as seen in Figure S6 at Supporting Information. These opposite charges of MB and Ti_2C lead to attractive electrostatic interaction.

Evaluation on the FRR of the membranes shows that antifouling of all membranes all relatively high. The ion of chloride salt can be retained in the membrane channel, affecting the membrane fouling. In addition, the fouling is also influenced by the membrane hydrophilicity, which can enhance the fouling resistance of the membrane (Umam et al., 2023). The hydrophilicity of the membrane surface accelerates the formation of a water layer on the membrane surface. This water layer is beneficial due to its ability to prevent clogging in membrane pores so that the permeability of the membrane will increase with the lower fouling of the membrane(A. L. Ahmad et al., 2019; Kadja et al., 2023). Overall, the FRR of all membranes is about >80%. Moreover, the decrease in rejection of the membrane was tested at 2-cycle filtration, as shown in Table S1. It can be seen that at two cycles, the rejection of the membrane decreases between 42.63-28.31% relative to the rejection at the first cycle. The result can be correlated with the capacity of the surface of the membrane to trap the dye removal decrease after 1st cycle of filtration. In addition, XRD analysis was done after the filtration process, as seen in Figure S7. This result shows that the peak of all membranes does not change significantly, which indicates the structure doesn't change after the filtration process. The MXM and MXM-S performed remarkably well due to the higher flux than the other previous work. The MXene and other nanomaterials have been used in membrane applications. Figure 4(d) shows the membrane filtration of prior studies, and the data was tabulated in Table S2. For instance, MCM 0.6 has been used for MB filtration with the rejection of 100%, while the flux is only about 44.97 L m^{-2} h^{-1} (Zhang et al., 2019). Thus, the result of this study has an outstanding performance.

Conclusion

The investigation of the MXene-based membrane was conducted in this work, including Ti_2C synthesis from Ti_2AlC phase, fabricated MXene-based membrane, modification Ti_2C with chloride salt (NaCl, KCl, $MgCl_2$, and $CaCl_2$), characterization, and membrane filtration test for methylene blue removal. Ti_2C has been successfully synthesized using in-situ HF as indicated by the absence of Al peak in XRD pattern and (002) plane shifted into a lower 2θ. Other analyses such as Raman, FTIR, and SEM also prove the transformation of Ti_2AlC to Ti_2C. Chloride salt modification of Ti2C increases the interlayer spacing by replacing Li+ as an intercalant with cationic salt (Na+, K+, Mg2+, and Ca2+). In addition, the

water contact angle of the membrane decreases with the addition of chloride salt, indicating that the membrane exhibits high hydrophilicity. As a result, all membranes have a high dye removal with a rejection of about >97%. Moreover, chloride salt could enhance the permeability of membranes than pure MXene-based membranes due to the greater interlayer spacing than Ti2C without chloride salt modification. MXM-KCl showed excellent performance compared to other membranes with outstanding flux and rejection of 3303.31 L m-2 h-1 and 99.01%, respectively. Besides that, the MXM-KCl has antifouling properties with an FRR of 94.47%, and the others have an FRR of about ~90%. Overall, the modification of the chloride salt of Ti_2C will elevate the membrane's performance and inhibit the trade-off effect of the membrane. This study revealed the potential of chloride salt-modified Ti_2C in membrane application. In terms of scalability, the used HF *in situ* in Ti_2C synthesis is a major challenge because it produces a small amount of HF in the final process. Therefore, it is highly recommended to use safe methods, such as molten salt etching, electrochemical etching, or alkali etching. In addition, computational studies and modelling using machine learning are highly recommended to be implemented to estimate the membrane performance.

Acknowledgement

This research was fully supported by Kurita Asia Research Grand 2022 provided by Kurita Water Environment Foundation and ITB-NTUST Joint Research Program 2023.

Compliance with ethics guidelines

The authors declare they have no conflict of interest or financial conflicts to disclose.

This article contains no studies with human or animal subjects performed by the authors.

References

Adapa, S., & Malani, A. (2018). Role of hydration energy and co-ions association on monovalent and divalent cations adsorption at mica-aqueous interface. *Scientific Reports, 8*(1), 12198. https://doi.org/10.1038/s41598-018-30549-9

Ahmad, A. L., Pang, W. Y., Mohd Shafie, Z. M. H., & Zaulkiflee, N. D. (2019). PES/PVP/TiO2 mixed matrix hollow fiber membrane with antifouling properties for humic acid removal. *Journal of Water Process Engineering, 31*, 100827. https://doi.org/10.1016/j.jwpe.2019.100827

Ahmad, H., Mohd Makhfuz, M. J., Yusoff, N., Azam, A. D., & Samion, M. Z. (2023). Synthesis of 2D titanium carbide Ti2C, its characteristics, and nonlinear optical properties. *Optical Materials, 135*, 113340. https://doi.org/10.1016/j.optmat.2022.113340

Al-Hamadani, Y. A. J., Jun, B.-M., Yoon, M., Taheri-Qazvini, N., Snyder, S. A., Jang, M., Heo, J., & Yoon, Y. (2020). Applications of MXene-based membranes in water purification: A review. *Chemosphere, 254*, 126821. https://doi.org/10.1016/j.chemosphere.2020.126821

Berdiyorov, G. R., & Mahmoud, K. A. (2017). Effect of surface termination on ion intercalation selectivity of bilayer Ti 3 C 2 T 2 (T = F, O and OH) MXene. *Applied Surface Science, 416*, 725–730. https://doi.org/10.1016/j.apsusc.2017.04.195

Din, M. I., Khalid, R., Najeeb, J., & Hussain, Z. (2021). Fundamentals and photocatalysis of methylene blue dye using various nanocatalytic assemblies- a critical review. *Journal of Cleaner Production, 298*, 126567. https://doi.org/10.1016/j.jclepro.2021.126567

Gautam, S., Agrawal, H., Thakur, M., Akbari, A., Sharda, H., Kaur, R., & Amini, M. (2020). Metal oxides and metal organic frameworks for the photocatalytic degradation: A review. *Journal of Environmental Chemical Engineering, 8*(3), 103726. https://doi.org/10.1016/j.jece.2020.103726

Gogotsi, Y., & Anasori, B. (2019). The Rise of MXenes. *ACS Nano, 13*(8), 8491–8494. https://doi.org/10.1021/acsnano.9b06394

Haider, S., Uddin Khan, S., Najeeb, J., Naeem, S., Rafique, H., Munir, H., Al-Masry, W. A., & Nazar, M. F. (2022). Synthesis of cadmium oxide nanostructures by using Dalbergia sissoo for response surface methodology based photocatalytic degradation of methylene blue. *Journal of Cleaner Production, 365*, 132822. https://doi.org/10.1016/j.jclepro.2022.132822

Halim, J., Persson, I., Moon, E. J., Kühne, P., Darakchieva, V., Persson, P. O. Å., Eklund, P., Rosen, J., & Barsoum, M. W. (2019). Electronic and optical characterization of 2D Ti 2 C and Nb 2 C (MXene) thin films. *Journal of Physics: Condensed Matter, 31*(16), 165301. https://doi.org/10.1088/1361-648X/ab00a2

DOI: 10.5614/j.eng.technol.sci.2026.58.4.1

Ibrahim, Y., Meslam, M., Eid, K., Salah, B., Abdullah, A. M., Ozoemena, K. I., Elzatahry, A., Sharaf, M. A., & Sillanpää, M. (2022). A review of MXenes as emergent materials for dye removal from wastewater. *Separation and Purification Technology, 282*, 120083. https://doi.org/10.1016/j.seppur.2021.120083

Jabbar, Z. H., Graimed, B. H., Okab, A. A., Issa, M. A., Ammar, S. H., Khadim, H. J., & Shafiq, Y. A. (2023). A review study summarizes the main characterization techniques of nano-composite photocatalysts and their applications in photodegradation of organic pollutants. Environmental Nanotechnology, *Monitoring & Management, 19,* 100765. https://doi.org/10.1016/j.enmm.2022.100765

Kadja, G. T. M., Dwihermiati, E., Sagita, F., Mukhoibibah, K., Umam, K., Ledyastuti, M., & Radiman, C. L. (2023). Mercapto functionalized–natural zeolites/PVDF mixed matrix membrane for enhanced removal of methylene blue. *Inorganic Chemistry Communications, 157,* 111263. https://doi.org/10.1016/j.inoche.2023.111263

Karahan, H. E., Goh, K., Zhang, C. (John), Yang, E., Yıldırım, C., Chuah, C. Y., Ahunbay, M. G., Lee, J., Tantekin‐Ersolmaz, Ş. B., Chen, Y., & Bae, T. (2020). MXene Materials for Designing Advanced Separation Membranes. *Advanced Materials, 32*(29), 1906697. https://doi.org/10.1002/adma.201906697

Kishor, R., Purchase, D., Saratale, G. D., Saratale, R. G., Ferreira, L. F. R., Bilal, M., Chandra, R., & Bharagava, R. N. (2021). Ecotoxicological and health concerns of persistent coloring pollutants of textile industry wastewater and treatment approaches for environmental safety. *Journal of Environmental Chemical Engineering, 9*(2), 105012. https://doi.org/10.1016/j.jece.2020.105012

Kumar, J., Justa, P., Jaswal, N., Kumar, H., Pani, B., & Kumar, P. (2024). Peroxidase like activity of Prussian blue nanoparticles and visible light mediated catalytic degradation of methylene blue dye. *Chemical Physics Impact, 8*(June 2024),100575. https://doi.org/10.1016/j.chphi.2024.100575

Lan, L., Fan, X., Yu, S., Gao, J., Zhao, C., Hao, Q., & Qiu, T. (2022). Flexible Two-Dimensional Vanadium Carbide MXene-Based Membranes with Ultra-Rapid Molecular Enrichment for Surface-Enhanced Raman Scattering. *ACS Applied Materials & Interfaces, 14*(35), 40427–40436. https://doi.org/10.1021/acsami.2c10800

Li, J., & Wang, F. (2017). Accurate Prediction of the Hydration Free Energies of 20 Salts through Adaptive Force Matching and the Proper Comparison with Experimental References. *The Journal of Physical Chemistry B, 121*(27), 6637–6645. https://doi.org/10.1021/acs.jpcb.7b04618

Li, L., Wang, F., Zhu, J., & Wu, W. (2017). The facile synthesis of layered Ti 2 C MXene/carbon nanotube composite paper with enhanced electrochemical properties. *Dalton Transactions, 46*(43), 14880–14887. https://doi.org/10.1039/C7DT02688A

Li, Y., Zhou, X., Wang, J., Deng, Q., Li, M., Du, S., Han, Y.-H., Lee, J., & Huang, Q. (2017). Facile preparation of in situ coated Ti 3 C 2 T x /Ni 0.5 Zn 0.5 Fe 2 O 4 composites and their electromagnetic performance. *RSC Advances, 7*(40), 24698–24708. https://doi.org/10.1039/C7RA03402D

Manzoor, K., Batool, M., Naz, F., Nazar, M. F., Hameed, B. H., & Zafar, M. N. (2024). A comprehensive review on application of plant-based bioadsorbents for Congo red removal. *Biomass Conversion and Biorefinery, 14(*4), 4511–4537. https://doi.org/10.1007/s13399-022-02741-5

Melchior, S. A., Raju, K., Ike, I. S., Erasmus, R. M., Kabongo, G., Sigalas, I., Iyuke, S. E., & Ozoemena, K. I. (2018). High-Voltage Symmetric Supercapacitor Based on 2D Titanium Carbide (MXene, Ti 2 CT x)/Carbon Nanosphere Composites in a Neutral Aqueous Electrolyte. *Journal of The Electrochemical Society, 165*(3), A501–A511. https://doi.org/10.1149/2.0401803jes

Naguib, M., Kurtoglu, M., Presser, V., Lu, J., Niu, J., Heon, M., Hultman, L., Gogotsi, Y., & Barsoum, M. W. (2011). Two-Dimensional Nanocrystals Produced by Exfoliation of Ti 3 AlC 2. *Adv. Mater., 23*, 4248–4253. https://doi.org/10.1002/adma.201102306

Naseem, K., Aziz, A., Anwar, A., Ameen, A., Faizan Nazar, M., Haider, S., & Saeed Akhtar, M. (2023). Role of bioinorganic metal nanoparticles as catalyst for the treatment of dyes polluted wastewater. *Inorganic Chemistry Communications, 157*, 111370. https://doi.org/10.1016/j.inoche.2023.111370

Naseem, K., Wakeel Manj, Q., Akram, S., Shabbir, S., Noor, A., Farooqi, Z. H., Urooge Khan, S., Ali, M., Faizan Nazar, M., Haider, S., & Alam, K. (2024). Spectroscopic monitoring of polyurethane-based nanocomposite as a potential catalyst for the reduction of dyes. *Spectrochimica Acta Part A: Molecular and Biomolecular Spectroscopy, 317*, 124450. https://doi.org/10.1016/j.saa.2024.124450

Oladoye, P. O., Ajiboye, T. O., Omotola, E. O., & Oyewola, O. J. (2022). Methylene blue dye: Toxicity and potential elimination technology from wastewater. *Results in Engineering, 16*, 100678. https://doi.org/10.1016/j.rineng.2022.100678

Priyadharsini, P., SundarRajan, P., Pavithra, K. G., Naveen, S., SanjayKumar, S., Gnanaprakash, D., Arun, J., & Pugazhendhi, A. (2023). Nanohybrid photocatalysts in dye (Colorants) wastewater treatment: Recent trends in simultaneous dye degradation, hydrogen production, storage and transport feasibility. *Journal of Cleaner Production, 426*, 139180. https://doi.org/10.1016/j.jclepro.2023.139180

Sagita, F., Mukhoibibah, K., Lestari, W. W., Patah, A., Radiman, C. L., & Kadja, G. T. M. (2024). Fast and highly selective anionic azo dye removal over unique PVDF/MIL-100(Cr) mixed matrix membranes. *Journal of Hazardous Materials Letters, 5*, 100107. https://doi.org/10.1016/j.hazl.2024.100107

Sagita, F., Radiman, C. L., Ledyastuti, M., Khalil, M., & Kadja, G. T. M. (2022). Salt-modified MXene membrane for ultrafast and efficient cationic and anionic dyes removal. *Journal of Water Process Engineering, 49*, 103133. https://doi.org/10.1016/j.jwpe.2022.103133

Schmid, R., Miah, A. M., & Sapunov, V. N. (2000). A new table of the thermodynamic quantities of ionic hydration: values and some applications (enthalpy–entropy compensation and Born radii). *Physical Chemistry Chemical Physics, 2*(1), 97–102. https://doi.org/10.1039/a907160a

Umam, K., Sagita, F., Pramono, E., Ledyastuti, M., Kadja, G. T. M., & Radiman, C. L. (2023). Polyvinylidenefluoride (PVDF)/surface functionalized-mordenite mixed matrix membrane for congo red dyes removal: Effect of types of organosilane. *JCIS Open, 11*, 100093. https://doi.org/10.1016/j.jciso.2023.100093

Wei, S., Xie, Y., Xing, Y., Wang, L., Ye, H., Xiong, X., Wang, S., & Han, K. (2019). Two-dimensional graphene Oxide/MXene composite lamellar membranes for efficient solvent permeation and molecular separation. *Journal of Membrane Science, 582*, 414–422. https://doi.org/10.1016/j.memsci.2019.03.085

Zafar, S., Sultan Rana, A., Ud-Din Khan, S., Haider, S., Ud-Din Khan, S., Haider, A., Ur Rehman, S., Ali, M., Nazeer, M., & Faizan Nazar, M. (2024). Photocatalytic membranes as water decontamination agents. Inorganic *Chemistry Communications, 170*, 113522. https://doi.org/10.1016/j.inoche.2024.113522

Zhang, S., Liao, S., Qi, F., Liu, R., Xiao, T., Hu, J., Li, K., Wang, R., & Min, Y. (2019). Direct deposition of two-dimensional MXene nanosheets on commercially available fi lter for fast and e ffi cient dye removal. *Journal of Hazardous Materials, 384*, July, 121367. https://doi.org/10.1016/j.jhazmat.2019.121367

Zhao, J., Liu, H., Xue, P., Tian, S., Sun, S., & Lv, X. (2021). Highly-efficient PVDF adsorptive membrane filtration based on chitosan@CNTs-COOH simultaneous removal of anionic and cationic dyes. *Carbohydrate Polymers, 274*, 118664. https://doi.org/10.1016/j.carbpol.2021.118664

Zheng, Y., Zhang, H., Yu, S., Zhou, H., Chen, W., & Yang, J. (2024). Covalently bridged MXene/COF hybrid membrane toward efficient dye separation. *Separation and Purification Technology, 349*, 127908. https://doi.org/10.1016/j.seppur.2024.127908

Manuscript Received: 11 February 2025
Revised Manuscript Received: 1 May 2025
Accepted Manuscript: 4 December 2025